Effect of Surface Finish on Wettability and Bacterial Adhesion of Micromachined Biomaterials

Santhosh Kumar S.[a], Somashekhar S. Hiremath[a,*], Balaji Ramachandran[b], Vignesh Muthuvijayan[b]

[a] Precision Engineering and Instrumentation Laboratory, Department of Mechanical Engineering, Indian Institute of Technology, Madras 600036, India
[b] Department of Biotechnology, Bhupat and Jyoti Mehta School of Biosciences, Indian Institute of Technology, Madras 600036, India

ABSTRACT

Bacterial infection is one of the major complications occurs in biomedical implants. Bacterial adhesion on the implant surfaces can form a biofilm, which leads to infection and failure at an earlier phase of implantation. So the surface properties of the implant such as surface topography, surface energy, and chemistry play a crucial role in bacterial adhesion. For decades, several surface finishing techniques have been developed to alter the surface properties in turn to reduce the bacterial adhesion. Most of these implants exhibit freeform surfaces which are difficult to finish with available finishing methods to obtain the uniform surface properties. The current paper focused on the development of a unidirectional abrasive flow finishing process used to finish biomaterials- stainless steel (SS316L) and titanium alloy (Ti-6Al-4 V ELI) with two different abrasive media and a varying number of cycles. The purpose of this study is to evaluate the effect of this finishing process on enhancing the surface characteristics like surface finish, surface topography and its role on wettability and initial bacterial adhesion. Optical profilometer and a scanning electron microscope are used to examine the surface topography and surface morphology of the finished surfaces. The goniometer is used to study the wettability of the finished samples using the sessile drop technique. Further, for the bacterial adhesion study both Gram-negative *Escherichia coli* (*E. coli*) and Gram-positive *Staphylococcus aureus* (*S. aureus*) are selected because these bacterial strains were commonly found on implant-related infections. The obtained result shows that, the surface finish and topography influences on wettability and bacterial adhesion. In conclusion, these results demonstrate that the possibilities of the developed process to enhance the surface finish of the biomedical implants which in turn reduce the implant-related infections and chances of early phase implant failure.

1. Introduction

1.1. Bacterial Infection on Orthopedic Implants

Orthopedic joint implants such as hip, knee, shoulder, ankle and elbow prosthesis are used for hard tissue replacement. These are load-bearing joints subjected to high levels of mechanical stress, fatigue and wear in the normal daily activities of humans. The artificial implants used for these applications should possess structural integrity as well as surface compatibility with the surrounding biological environment for prolonged survivability without complications [1–4]. Despite the adoption of advanced technology in manufacturing new implants and in surgical and medical management procedures, there are still a large number of implants that are subject to infection [5]. The major causes for implants failure are a fracture, prosthetic dislocation, loosening, excessive wear rate at mating surfaces and its associated debris

(although this cause has been much reduced by the use of cross-linked polyethylene) and pre-surgical contamination/infection (i.e. bacterial adhesion). The American Joint Replacement Registry Annual Report 2018 collected data between 2012 and 2017 and showed that 8.2% of 47,378 hip arthroplasty revisions and 7.9% of 40,488 knee arthroplasty revisions were due to the infection and inflammatory reactions. The National Joint Registry for England, Wales, Northern Ireland and the Isle of Man for 2018 report showed that 0.72% of all hip replacements, 0.93% of all knee replacements and 6% of all shoulder replacements had implants-related infections. Similarly, it was reported in the Australian Orthopedic Association National Joint Replacement Registry (AOA NJRR) Annual Report 2018 that overall < 1% of knee and hip arthroplasties had to be revised due to infection. In the present study, a focus has been made on the relation between the surface roughness and the bacterial adhesion which is critically important from a clinical perspective when surfaces are made with a finishing process.
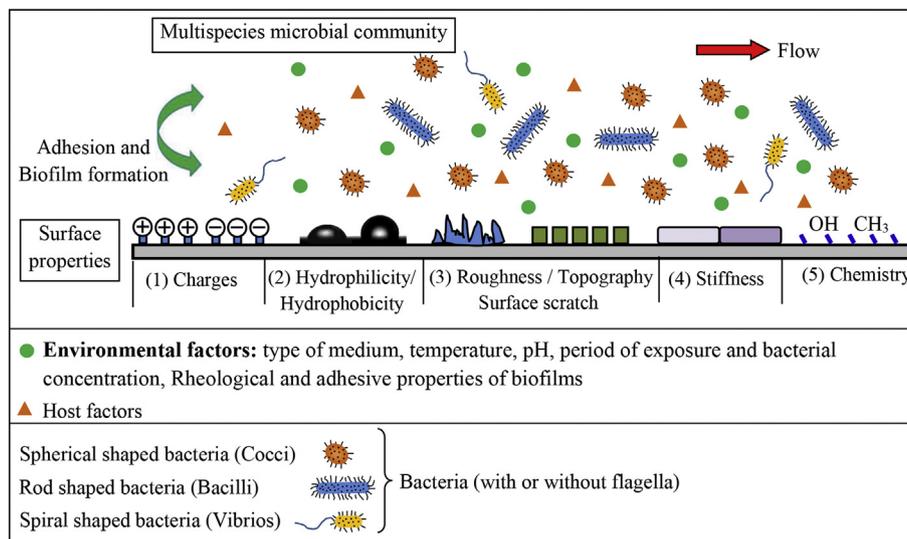

Fig. 1. Schematic diagram of bacterial adhesion and the effect of implant material properties [12].

Bacterial infections on implants are usually initiated through adhesion of bacteria to the implant surface by means of physiochemical interaction between the implant surface and bacteria i.e. van der waals forces, electrostatic forces and gravitational forces [6,7]. The reversible bacterial adhesion is followed by colonization and formation of biofilm which forms a layer of bacteria binding irreversibly to the implant surface which is later difficult to remove from implants [7,8]. The bacterial adhesion on the implant surface depends on the (1) properties of the implant material such as surface topography, surface roughness, surface chemistry and surface energy (2) properties of the bacteria such as surface charge, surface hydrophobicity (contact angle, θ > 90°) / hydrophilicity (contact angle, θ < 90°) and appendages and (3) properties of the surrounding environment such as type of antibiotics and associated flow condition, temperature, pH value, period of exposure, chemical treatment and bacterial concentration. Fig. 1 shows the schematic diagram of bacterial adhesion and the effects of implant material properties. In particular, surface roughness and topography are most influencing parameters because studies show that surface roughness increase the surface area of the material and also the depression, grooves, pits, scratches and crevices in the rough surfaces influences the bacterial adhesion and acts as favorable sites for colonization and biofilm formation [2,9–11].

The near-net-shape of the bioimplants with the required surface finish is achieved by various finishing steps after the primary machining process. After the pre-fabrication, implants are subjected to the grinding process at the end. Final finishing of these surfaces is performed using polishing integrated with multi-axis CNC machines, vibratory abrasive polishing, free abrasive polishing, fixed abrasive polishing, belt polishing, etc., which have all been comprehensively used in the past decades [11,13–15] to remove the finer irregularities. It was estimated that polishing processes typically accounted for 10%–15% of the total manufacturing cost and detailed review on different manufacturing and finishing processes used in implant manufacturing are detailed in a study conducted by Kang and Fang [15]. Most of the implants have a complex and partly freeform surface which raises the difficulty in finishing at one step and also one should have the knowledge of frequently changing contact condition while performing finishing operation. There is a need for a technique which can be used to finish the complex surfaces of orthopedic implants without changing its contact condition and without disturbing the dimensional accuracy. Abrasive flow finishing is one such process, in which flexible abrasive media is used to finish the complex surfaces. Previous studies have demonstrated that this process has capable of finishing complex

internal and external surfaces and also freeform surfaces with controlled surface topography without disturbing the dimensional accuracy [16–21]. Although there have been studies on the finishing of freeform surfaces using this process, understanding the biocompatibility of surfaces finished with this process is still far from the complete study. In this work different variant of abrasive flow finishing process i.e. unidirectional abrasive flow finishing process is developed and working of this process is explained in the next section.

1.2. Unidirectional Abrasive Flow Finishing Processes

The unidirectional abrasive flow finishing process is proposed to finish biomaterials in the present work. A flexible abrasive medium which is a combination of viscoelastic polymer, abrasive particles and plasticizer are used to finish any type of complex internal and external surfaces using the developed setup. The typical system consists of an abrasive media cylinder in which the abrasive media is filled and coupled to the hydraulic cylinder which is controlled by 4/3 solenoid operated directional control valve and hydraulic power pack connected through the flexible hoses. The hydraulic cylinder is driven through the hydraulic power pack to give the linear movement to push the abrasive media present in the abrasive media cylinder through the workpiece to be finished. The samples are fixed rigidly at the exit of the abrasive cylinder using the developed fixture designed to hold four samples at one time shown in Fig. 2 (a). This cycle repeats until the required surface finish is achieved on the work surfaces.

Fig. 2 (b) shows the material removal mechanism. The abrasive media extruded over the workpiece surfaces removes the irregularities left over the surfaces (from the earlier process) in the form of micro/nanochips for every cycle. During the movement of abrasive media for each cycle, the height of the peak will gradually decrease and finally, a surface gets a mirror-like finish. The micro-cutting mechanism involves two force components: (a) radial force due to elastic component of media responsible for penetrating particle inside the workpiece and (b) shear force or axial force due to the viscous component of the media responsible for shearing of material as penetrated above along the direction of applied pressure and abrades the work surface in the form of layer by layer (microchips).

Hence, the material removal mechanism includes three deformation modes – elastic deformation, plastic deformation and micro cutting of the material. These are influenced by rheological properties of abrasive media (shear viscosity, shear stress, loss modulus, storage modulus, complex viscosity), type of abrasives (SiC, Al_2O_3, B_4C) and
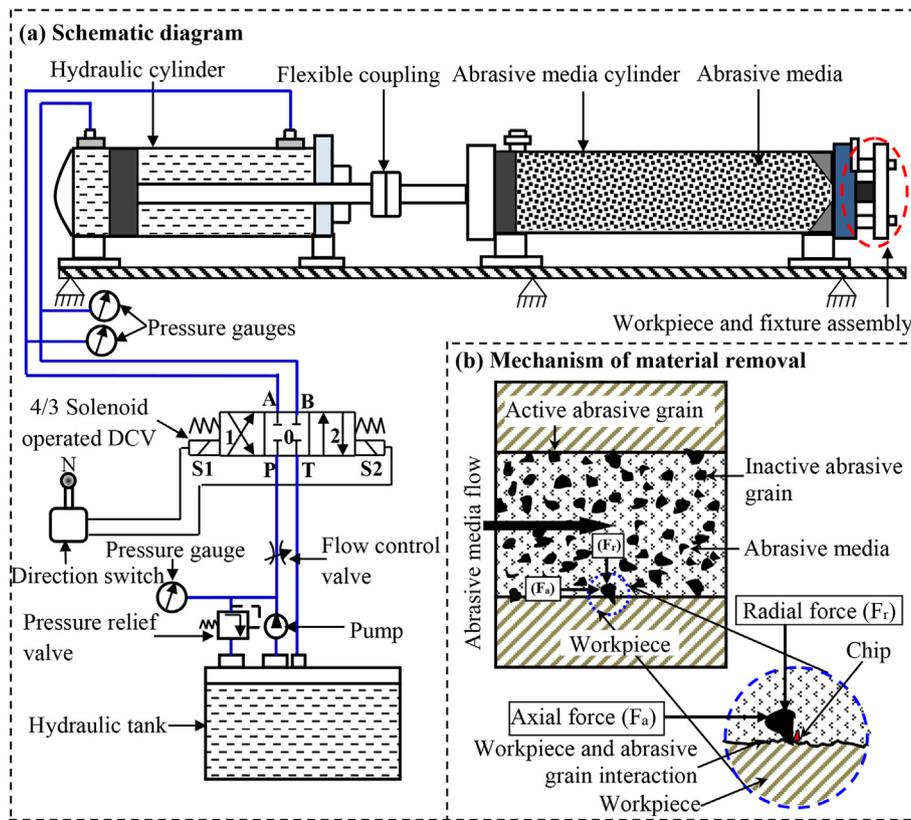
Fig. 2. Schematic diagram showing working principle of unidirectional abrasive flow finishing process.

concentration used, type of polymer (viscoelastic polymer) and concentration used, number of processing cycles, extrusion pressure (10 bar – 100 bar), fixture design, workpiece material, plasticizer and operating condition. The major advantage of this process is, it can finish any type of surfaces - freeform surfaces, complex internal cavities, and complex external surfaces without damaging the surface due to the flexibility of the media which has the ability to take the shape of the component during the finishing process. This cannot be achieved with conventional finishing processes like grinding, lapping and honing due to the restriction of the tool to reach the complex surfaces.

The present work aims at in-house development of unidirectional abrasive flow finishing process to finish the two widely used biomaterials - stainless steel – SS316L and titanium alloy – Ti-6Al-4 V ELI. Viscoelastic polymer-based abrasive media which is a mixture of a known quantity of viscoelastic polymer, plasticizer and abrasive particles mixed thoroughly using two-roll mill method. Samples are finished with two different types of abrasive sizes - #220 and #400 and the number of cycles are varied from 3 to 6.

Further, the surface properties like surface roughness, surface morphology and the contact angle of the samples are characterized using a profilometer, scanning electron microscope and contact angle goniometer. Bacterial adhesion of both Gram-negative *Escherichia coli*

and Gram-positive *Staphylococcus aureus* on finished surfaces are investigated using colony-forming units count method. The main objectives of this work are (a) to develop the simple, economical and automated finishing process to finish biomaterials used for bacterial adhesion and (b) to investigate the influence of finishing parameters on material surface roughness, surface morphology, wettability on bacterial adhesion.

2. Materials and Methods

2.1. Materials and Abrasive Media

The materials are selected for bacterial adhesion based on ASTM F138 - Stainless steel SS316L [22] and ASTM F136 - Titanium alloy Ti-6Al-4 V ELI [23] are obtained from Auxein Medical Pvt. Ltd., Sonepat, India. Fig. 3 shows the sample and fixture assembly to hold the sample rigidly during the machining process. Circular disc type of samples is prepared with a dimension of 13 mm diameter and 6 mm thickness for measuring the roughness, contact angle, and bacterial adhesion study. In-house developed viscoelastic polymer based flexible abrasive media is used to finish the biomaterials. The media is a mixture of viscoelastic polymer (Silicone rubber – Grade: Bluesil HCR 1940 L A2, Bluestar
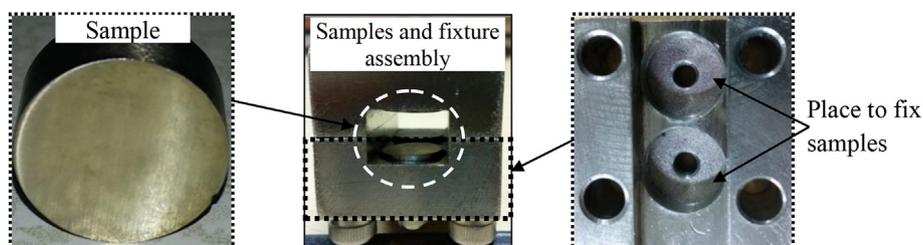

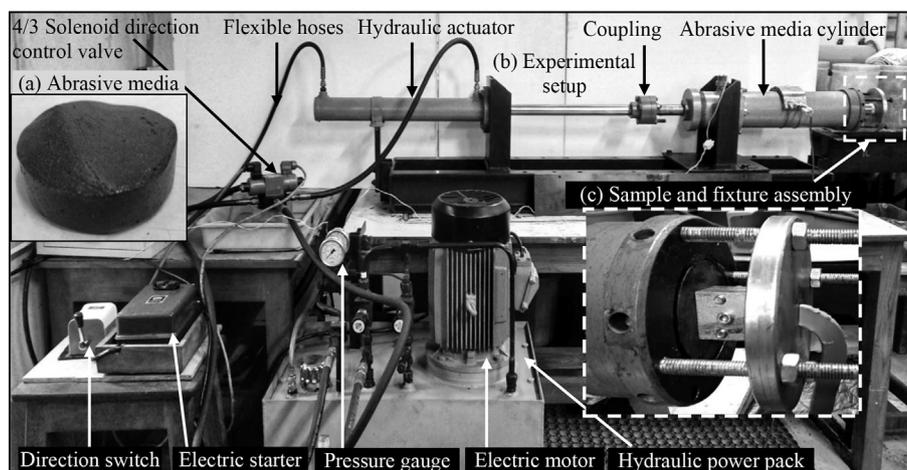
Fig. 3. Samples and fixture assembly.

Fig. 4. Photographic view of a unidirectional abrasive flow finishing process.

silicones, China), processing oil (Silicone oil – Grade: WACKER AK 1000, Wacker, India) impregnated with abrasive particles (Green SiC – #220 and #400, SNAM abrasives, India). The selected weight percentages of individual materials are 50% + 38% + 12% (Green SiC + Silicone rubber + Silicon oil) and mixed uniformly using two-roll mill process. The shape, size, and concentration of the abrasive particles are also deciding factors while machining. So in the present work, two types of abrasive media are used with different abrasive particles size #220 and #400. The average size of the abrasive particles found around 75 μm in 220 mesh size and 30 μm in 400 mesh size.

2.2. Finishing of Biomaterials

Fig. 4 shows the photographic view of a unidirectional abrasive flow finishing experimental setup used to finish the biomaterials and details on the working of the experimental setup is explained in Section 1.2. Table 1 shows the details of the experimental condition used during experimentation. The process parameters are selected based on preliminary work and previous work. A number of cycles of abrasive media and abrasive particle sizes are varied.

Table 1
Details of experimental conditions.

Parameters	Particulars			
Sample materials	(a) ASTM F138: SS316L			
	(b) ASTM F136: Ti-6Al-4 V ELI			
Sample size and shape	Circular disc: 13 mm diameter × 6 mm thickness			
Abrasive media	Type	Abrasive particles	Polymer	Plasticizer
	1	SiC #220	Silicone rubber	Silicone oil
	2	SiC #400	Silicone rubber	Silicone oil
Abrasive concentration	50% abrasive particles + 38% silicone rubber + 12% silicone oil			
Operating temperature	Room temperature (30 ℃)			
Working pressure	50 bar			
Sample details				
Sample	Mesh size	No. of cycles	Coding	
Sample 1	As-received	0	As-received	
Sample 2	220	3	220 - 3C	
Sample 3	220	6	220 - 6C	
Sample 4	400	3	400 - 3C	
Sample 5	400	6	400 - 6C	
Sample 6	220 and 400	3, 3	Hybrid	

2.3. Surface Characterization

Both surface roughness and a surface topography measurement of samples are performed using optical profilometer - Wyko NT1100 Veeco Instruments, USA. Five measurements on each sample and three independent replicates (3 samples) for each experiment are considered to ensure the repeatability and variation is represented with an error bar based on standard deviation.

Surface roughness parameters such as average surface roughness (R_a) and bearing area curve are analyzed. Further, the sessile drop technique is used to quantify the surface wettability of the finished surfaces, by obtaining the contact angle of water droplet on each surface using Goniometer device - GBX-Digidrop MCAT, Ireland. Initially, the surfaces are cleaned with distilled water and ultrasonicated for 15 min with ethanol using ultrasonicator to remove debris/dust particles, etc. The samples are dried at room temperature before taking the measurements. The droplet of 2 μL volume was placed on each sample using microsyringe and static droplet angle was measured at room temperature. The delay time of measurement in the experiment was set to be 20 s. Scanning Electron Microscope (SEM) is used to evaluate the morphology of samples and abrasive particle size and shape.

2.4. Bacterial Adhesion Study

For the bacterial adhesion assay, all the samples - SS316L and Ti-6Al-4 V ELI finished with different process parameters were placed in an individual well in 24-well plates. For each study, three independent samples are considered for counting bacterial adhesion and one sample is used for SEM analysis (total number of samples SS316L: 48 and Ti-6Al-4 V ELI: 48). The samples were washed with water, ethanol, and UV sterilized overnight to remove the contamination over the surfaces. Two different bacterial strains *Escherichia coli* (ATCC 25922) and *Staphylococcus aureus* (ATCC 25923) were used for this study as because these bacterial strains were commonly found on implant-related infections [2,10]. A single colony of the culture was inoculated into 50 mL Lysogeny broth (LB) medium and incubated at 37 ℃ with 180 rpm for growth. After the culture reached the logarithmic growth phase (Optical Density ≈ 0.4) confirmed with a spectrophotometer, 2 mL of the bacterial suspension were transferred into sample well plates and incubated for 12 h at 37 ℃ shown in Fig. 5. After incubation, the samples were carefully dipped in sterile phosphate buffer saline (PBS) twice to remove loosely bound bacteria and transferred to another sterile plate. Then the samples were sonicated in fresh LB broth to remove the adhered bacteria. Subsequently, the culture was serially diluted to reduce the concentration and spread plated on the LB agar plate for the growth of bacteria. After overnight incubation at 37 ℃, the viable colonies

(a) Ti-6Al-4V

(b) Bacterial suspension – *E. coli*

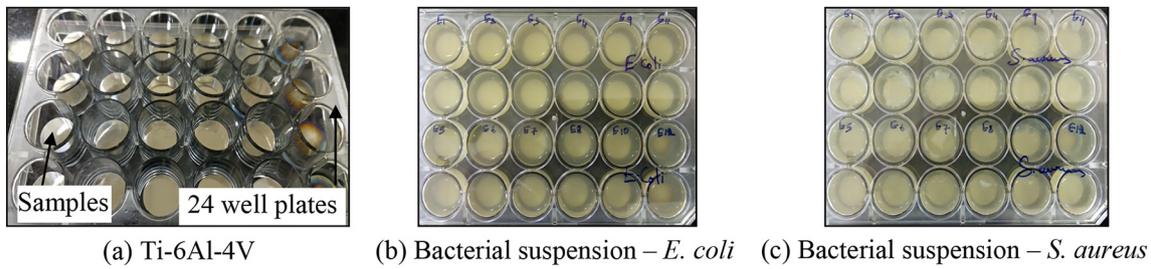(c) Bacterial suspension – *S. aureus*

Fig. 5. Samples with well plates.

were counted to calculate the colony-forming units (CFU) and expressed as a number of bacteria adhered on samples per mm^2.

The adhered bacteria on the surfaces were observed using SEM. Briefly, after PBS wash (to remove any nonadherent bacteria), the bacterial adhered samples were incubated in 2.5% glutaraldehyde for 2 h at 37 °C to fix the cells. Then, the samples were dehydrated with a series of ethanol concentrations in water (50%, 70%, 90%, and 100% vol.) for 15 min each to remove moisture content from the samples. After complete dehydration, the samples were gold coated and observed under SEM for analysis on bacterial adhesion.

2.5. Statistical Analysis

Statistical significant differences between as-received samples and finished surfaces are analyzed using one-way ANOVA on GraphPad Prism software. The experimental data are represented as a mean ± standard deviation with a number of replicates. Statistical significance is represented by p values: *p < 0.05 (significant), **p < 0.01 (very significant), ***p < 0.001, ****p < 0.0001 (extremely significant).

3. Results and Discussions

3.1. Finishing

Fig. 6 (a) shows a change in surface roughness of the SS316L with different finishing cycles. Initially, the average surface roughness (R_a) of the as-received samples was 463 nm ± 20 nm. After finishing with abrasive media of 220 mesh size at 3 cycles, average surface roughness reduced to 163 nm ± 15 nm and another 3 cycles reduced it to 113 nm ± 12 nm. For 400 mesh abrasive media initial surface roughness from 463 nm ± 20 nm reduced to 213 nm ± 20 nm roughness at 3 cycles and further reduced to 139 nm ± 10 nm roughness and significant differences were observed. Fig. 6 (b) shows a change in average surface roughness of the Ti-6Al-4 V ELI with different finishing cycles.

The surface roughness of as-received was 402 nm ± 18 nm. After

finishing with abrasive media of 220 mesh size at 3 cycles, surface roughness reduced to 160 nm ± 13 nm and another 3 cycles further reduced it to 120 nm ± 14 nm. For 400 mesh abrasive media, initial surface roughness from 463 nm ± 20 nm reduced to 223 nm ± 15 nm roughness at 3 cycles and further reduced to 143 nm ± 10 nm roughness. It is observed that during the first 3 cycles maximum roughness is removed, while in later 3 cycles the percentage of change in roughness is less.

This is due to the large density of peaks during initial cycles and later it was reduced as finishing process progress. Also, with respect to mesh size, 220 mesh size media takes less amount of time to remove the peaks compared to 400 mesh size media. This is due to the change in size shape of the abrasive particles which can be observed in SEM images Fig. 7 (a) and 7 (b). Fig. 7 (c) shows the SEM image of the abrasive media.

The average size of the abrasive particles in 220 mesh size media is 75 μm which is more compared to 400 mesh size media with an average particles size of 30 μm. In general finishing process, 220 mesh is used for rough finishing and 400 mesh used for fine finishing. Due to smaller size particles in 400 mesh media, takes more number of cycles to remove the larger peaks. In case of 220 mesh size, the particles size is more (75 μm) and takes less time to finish the surfaces but once the surface roughness reaches the critical value which cannot be finished by 220 mesh, then 400 mesh is preferred for further finishing to remove the finer peaks. So, based on the experiments conducted, one hybrid parameter (it can also be treated as multistage finishing) is considered to finish the surfaces and in turn to reduce the finishing time. Initially, 3 cycles are finished with 220 mesh media and next 3 cycles with 400 mesh media and achieved < 100 nm average surface roughness with the same number of cycles. The roughness is reduced to 68 nm ± 8 nm from 463 ± 20 in case of SS316L material and 73 nm ± 10 nm from 402 nm ± 18 nm in case of Ti-6Al-4 V ELI. Another main parameter which also has an impact on the finishing process is material hardness as because it is observed from the results, the percentage change in roughness is more in SS316L compare to Ti-6Al-4 V ELI as because the
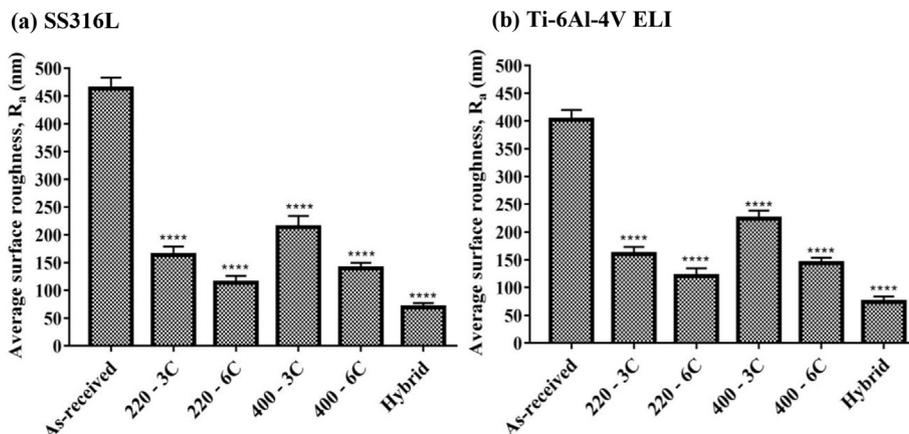
(a) SS316L

(b) Ti-6Al-4V ELI

Fig. 6. Variation of surface roughness with different process parameters (a) SS316L (b) Ti-6Al-4 V ELI.
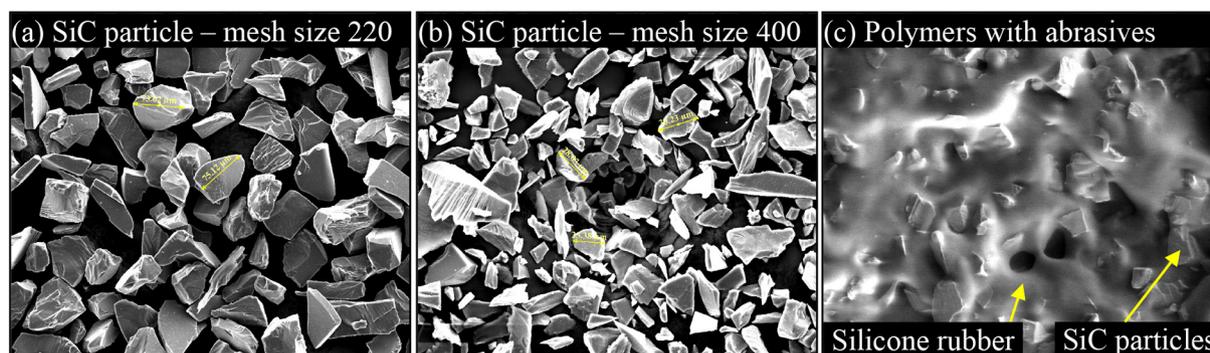
Fig. 7. SEM images of abrasive particles and mixed abrasive media.

hardness of the SS316L is less compared to Ti-6Al-4 V ELI material.

Fig. 8 shows the Profilometer images showing the surface topography of the surface before and after finishing with different process parameters. It shows the variation in peaks height with respect to changes in roughness. The roughness variations (peaks height) are more at received samples and as the finishing process progress, the variation is reduced for both the materials. Fig. 9 shows the morphology of as received and hybrid samples of SS316L and Ti-6Al-4 V ELI. Deep scratches and pits were present on the as-received samples are reduced after finishing and SEM images confirm the enhancement in surface finish.

Average surface roughness (R_a) value gives only the information about variation in the height of the irregularities but it does not give any information about sizes, slopes, and shapes of surface irregularities. Surfaces texture with linear grooves and crisscross grooves have an influence on the friction between the mating surfaces especially in bearing surfaces. A possible way to describe these type of surfaces using the Bearing Area Curve (BAC) also called Abbott–Firestone curve used for analysis of load carrying surfaces, bearing applications, adhesive and sealing properties [24]. In such applications, the topography of the surface must be established which can reduce the friction and enhance the life of mating surfaces. In the case of implants, the bearing area of the surface may be correlated with the biomechanical properties of the surface and the long-term anchoring of the implant [25–27]. BAC is used to show the quality of surface texture and also for a measured surface, it gives access to the size and proportions of the peaks and valleys present [24,28].

In the present work, an attempt has been made to show graphically BAC of SS316L and BAC of Ti-6Al-4 V ELI before and after finishing. Fig. 10 shows the bearing area curve for as received sample and samples finished with different abrasive media and cycles. In contrast to initial surfaces, the surfaces finished with a developed technique demonstrated a reduction in the density of peaks and valleys irrespective of the materials. Surface asperity – peaks of the surface finished with hybrid parameters is less compared to other surfaces and it got fewer irregularities.

3.2. Wetting Property

Besides the surface roughness, surface topographical features and surface morphology, hydrophobicity/hydrophilicity of implant surfaces are also known to influence the adhesion of bacteria on the surfaces [29,30]. Contact angle of the water droplet on SS316L and Ti-6Al-4 V ELI materials as a function of roughness are measured with contact angle Goniometer. Fig. 11 shows the variation of the contact angle for the two materials.

The contact angle of the as-received surface is 88.5° ± 3.6° after finishing it is increased to 102° for the surface finished with hybrid parameters. Similarly, for Ti-6Al-4 V ELI contact angle of the as-received surface was 83° ± 6° and it is increased to 96° ± 4°. It is observed from the results that, the as-received samples exhibit a lower contact angle than finished surfaces and shows significant changes after finishing.

3.3. Bacterial Adhesion

The bacterial adhesion on two types of material (SS316L and Ti-6AL-4 V ELI) surfaces finished with different process parameters are evaluated. We hypothesized that the decreased surface roughness by abrasive flow finishing will lead to reduced bacterial adhesion. Therefore, we explored the effect of physical characteristics, such as surface roughness and surface topography of the material surface on bacterial adhesion. Fig. 12 shows the adhesion of *E. coli* on SS316L and Ti-6AL-4 V ELI surfaces. For SS316L, the as-received sample had a bacterial count of 4.99×10^{10} CFU/mm^2 (Fig. 12 a). The decrease in surface roughness by varying finishing parameters tend to reduce bacterial adhesion. For hybrid parameter finishing, there is a significant reduction in a number of bacterial colonies (6.86×10^9 CFU/mm^2). A similar trend in bacterial reduction was observed in the case of Ti-6Al-4 V ELI as well (Fig. 12 b). The colonies reduced from 3.13×10^{10} CFU/mm^2 (as-received) to 6.53×10^8 CFU/mm^2 as the roughness decreased for the hybrid finished sample. Our data indicate that SS316L samples used, are more susceptible to bacterial adhesion compared to the Ti-6Al-4 V ELI samples. The possible reason might be that, the initial roughness range of titanium samples are less compared to the stainless steel samples. A similar trend was observed in *S. aureus* adhesion on both the samples (Fig. 13). The adhesion of *S. aureus* on SS316L surfaces reduced from 1.39×10^{11} CFU/mm^2 to 3.41×10^{10} CFU/mm^2 after hybrid finishing (Fig. 13a).

Similarly, Fig. 13 (b) shows the adhesion of *S. aureus* on Ti-6Al-4 V ELI reduced from 1.28×10^{11} CFU/mm^2 to 1.27×10^{10} CFU/mm^2. The results depict that, there were statistically significant differences in the total number of bacterias adhered to SS316L and Ti-6Al-4 V ELI between as received and finished surfaces. This may be due to reduced surface roughness and increased hydrophobicity of the finished surfaces. It is reported by Hauslich [32] that, increased adhesion of bacteria onto rough surfaces may be due to enlarged surface areas related to irregularities created during the manufacturing of these surfaces.

The quantity of *E. coli* adhesion on other finished surfaces was almost similar because the roughness value (R_a) of these surfaces were all in the range of below 200 nm. A similar observation is made in a study conducted by Quirynen et al. [29,31]. The surface roughness of 200 nm R_a is the threshold R_a below which, roughness does not have an effect on the bacterial adhesion. But for *S. aureus*, such correlations were not observed because significant variation in the bacterial adhesion is observed among the other finished surfaces. The colony count method was further supported by SEM images of bacterial adhesion on the material surfaces (Fig. 14).

Both the bacteria, *E. coli* and *S. aureus* adhesion decreased on finished (modified) surfaces compared to the as-received (unmodified)
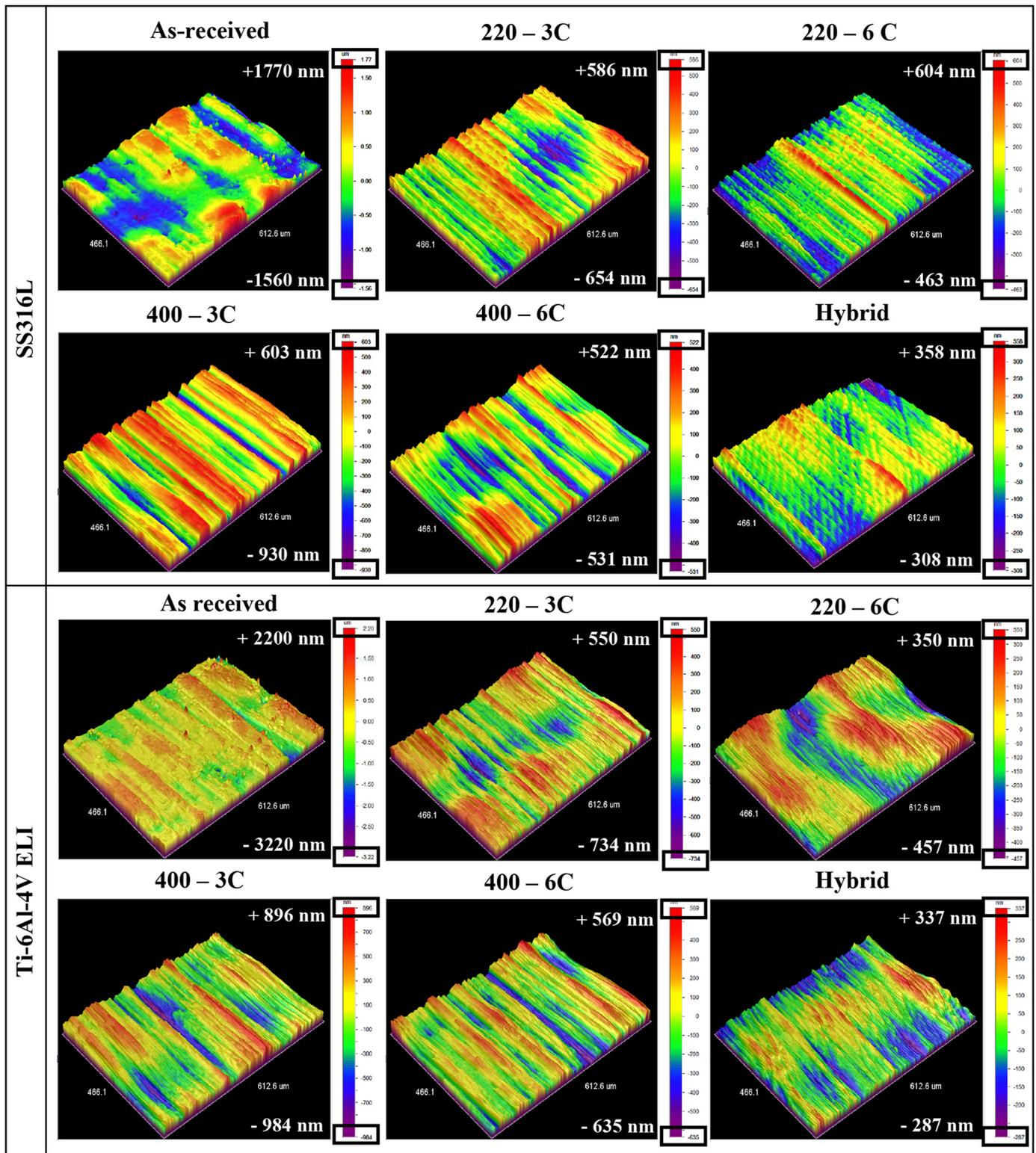
Fig. 8. Profilometer images showing the surface topography with different machining conditions.

surfaces. From the SEM images (Fig. 14) of the as-received sample of SS316L, it was clearly observed that *S. aureus* bacteria were found to be localized in the few crevices present on the surface. The amount of the bacterial colonies on the finished surfaces was less compared to the as-received surfaces. On some of the finished surfaces *E. coli* bacteria lay across the groove direction this may be due to the width and depth of the features were significantly smaller than the cells and similar type of observations are reported by Edwards et al. [35] and Mortimer et al.

[38]. Studies also show, bacteria are more susceptible to rough surface and it tends to accumulate more in concave features due to increased contact area [33]. Morphological description of the surface patterns such as grooved surface, braided surface, porous surface, and scratches have more influence on initial bacterial adhesion along with roughness parameters [2,34,35]. Even though the grooves are present on both the unmodified and modified surfaces, further analysis to be carried out to identify the reasons for the change in densities of bacterial adhesion.

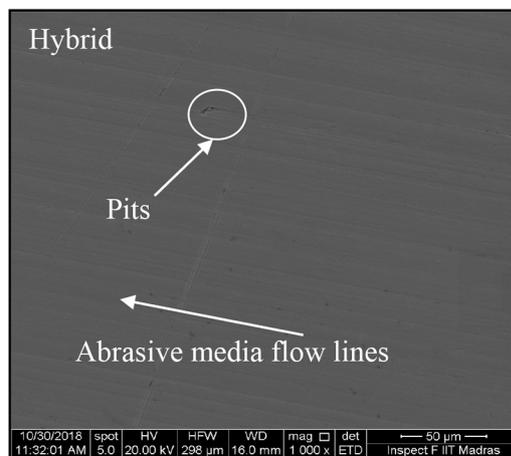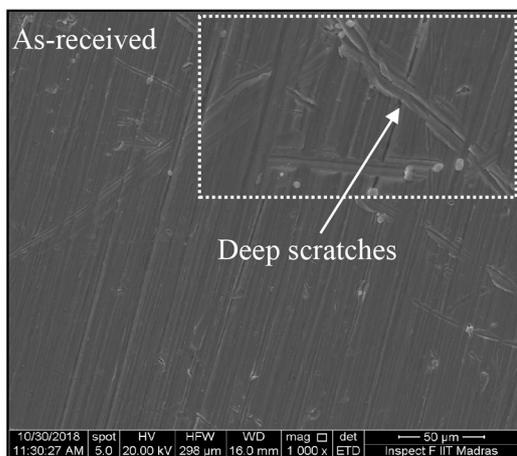**(a) SS316L**
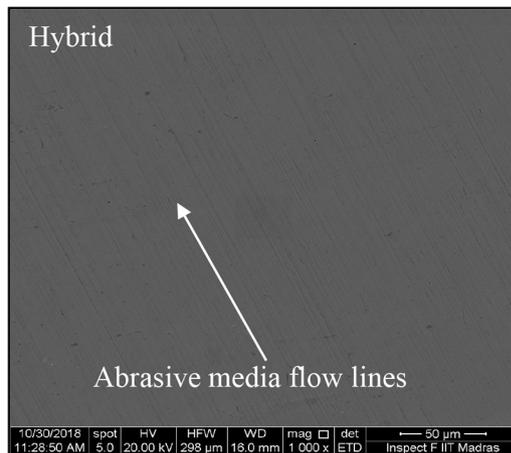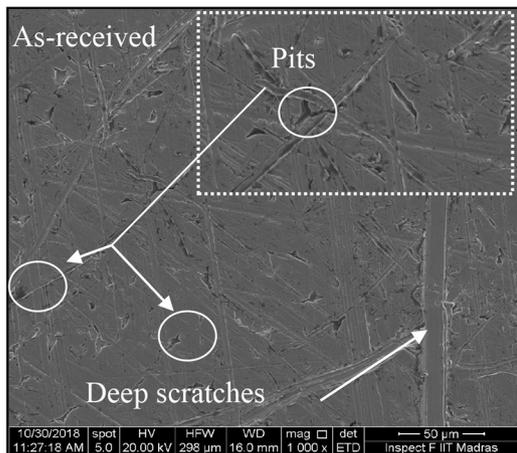
(b) Ti-6Al-4V ELI

Fig. 9. SEM images showing the morphology of the samples.

Fig. 15 shows the 2D roughness profile along X-axis and Y-axis for different surfaces. The X-axis shows the roughness profile perpendicular to the grooves and the Y-axis shows the roughness profile along the grooves. It is observed that for both the materials SS316L and Ti-6AL-4 V ELI, the as-received samples have few grooves with larger height and width (20 μm to 40 μm) and also appeared to be significantly irregular than the hybrid samples (finished samples) with smoother and smaller grooves. It could be that, these smaller-sized grooves could not possibly accommodate bacteria which have considerably larger in dimensions and bacterial colonies can be filled more in the grooves with a higher width than bacterial size [30,36,37]. It is also corroborated by the bearing area curve (Fig. 10), which shows that the volume of the peaks and valleys of as-received samples are higher than the finished samples. Having a low volume of peaks and valleys, reduce the
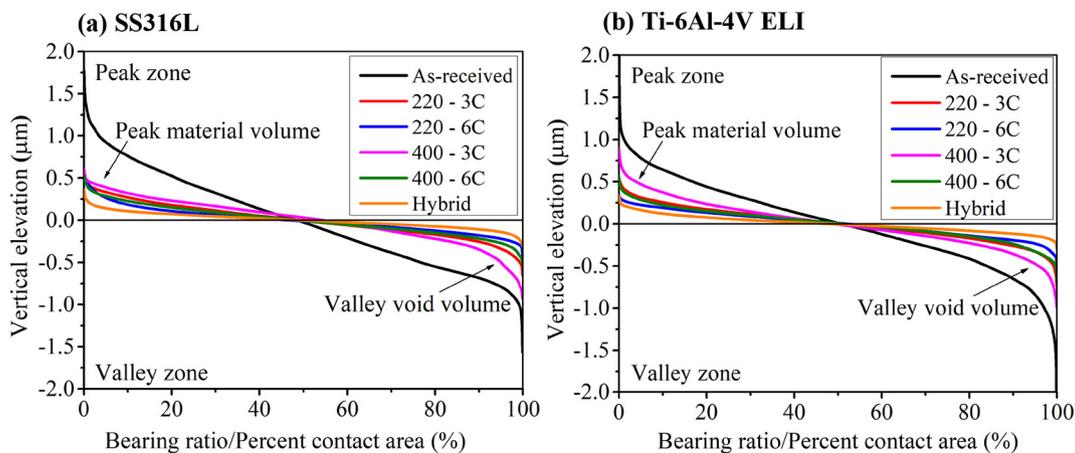

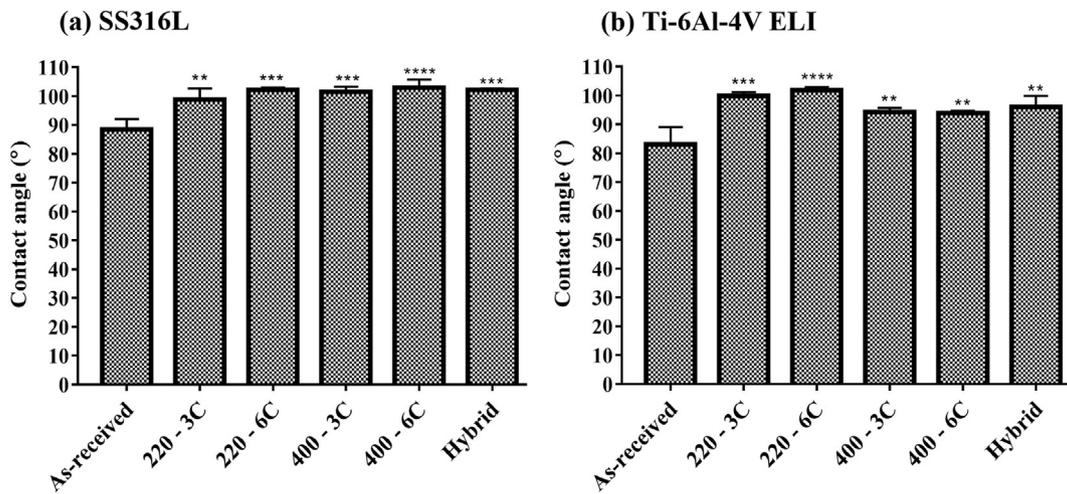Fig. 10. Bearing area curve of as-received and finished samples.

(a) SS316L

(b) Ti-6Al-4V ELI

Fig. 11. Contact angle variation for different samples.

(a) SS316L

(b) Ti-6Al-4V ELI

Fig. 12. *E. coli* adhesion on samples (*p < 0.05, **p < 0.01 ***p < 0.001 vs. as-received).

(a) SS316L

(b) Ti-6Al-4V ELI
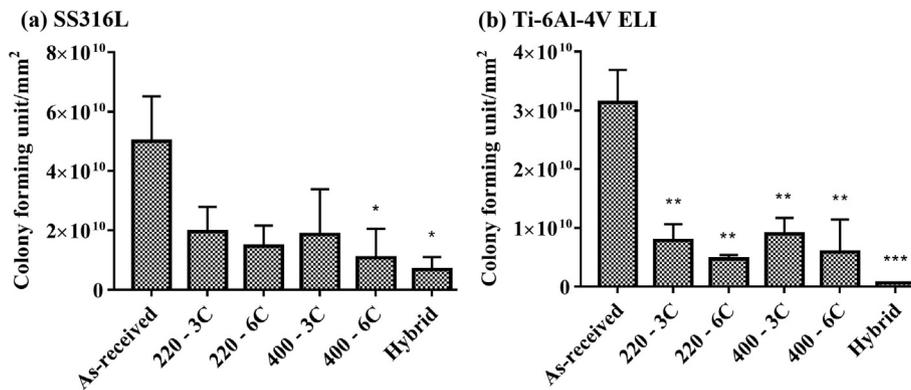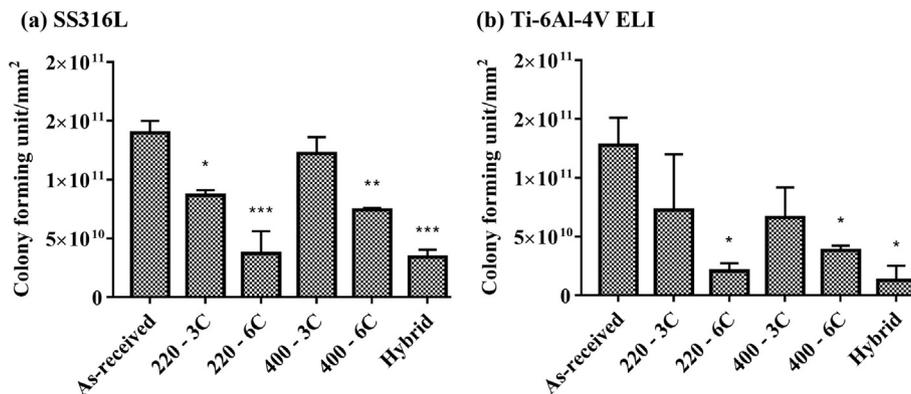
Fig. 13. *S. aureus* adhesion on samples (*p < 0.05, **p < 0.01 ***p < 0.001 vs. as-received).

accommodation of bacterial cells, while the higher volume on as-received samples favors the bacterial accommodation. The reduced bacterial adhesion on the finished work surface - SS316L and Ti-6Al-4 V ELI using unidirectional abrasive flow finishing shows that the developed process is effective and it calls for clinical verification on prosthetic implants to qualify for Prosthetic Implant Infection (PII).

Initial bacterial adhesion and biofilm formation is a multi-factor phenomenon as discussed in Section 1.1 and it is very difficult to conclude with few factors alone. Although the experimental results show the reduced bacterial adhesion on surfaces finished, several limitations must be noted when interpreting the results. There are other factors like bacterial surface characteristics and surrounding

environmental factors might have also influenced the bacterial adhesion. The main objective of this work is to characterize and identify the parameters to finish biomaterials using flexible abrasive media and to study its effect on bacterial adhesion. This work provides valuable insights on how the proposed finishing process can reduce the surface roughness and its effect on bacterial adhesion and the process adaptability for finishing orthopedic implants. However, limitations such as selection of abrasive media, designing fixture (based on the shape of the particular implant), surface cleaning of the device (after finishing process) and continues monitoring of the abrasive media are the challenges yet to overcome. Further tuning of process parameters to enhance the surface finish, the fretting wear and corrosion of the finished
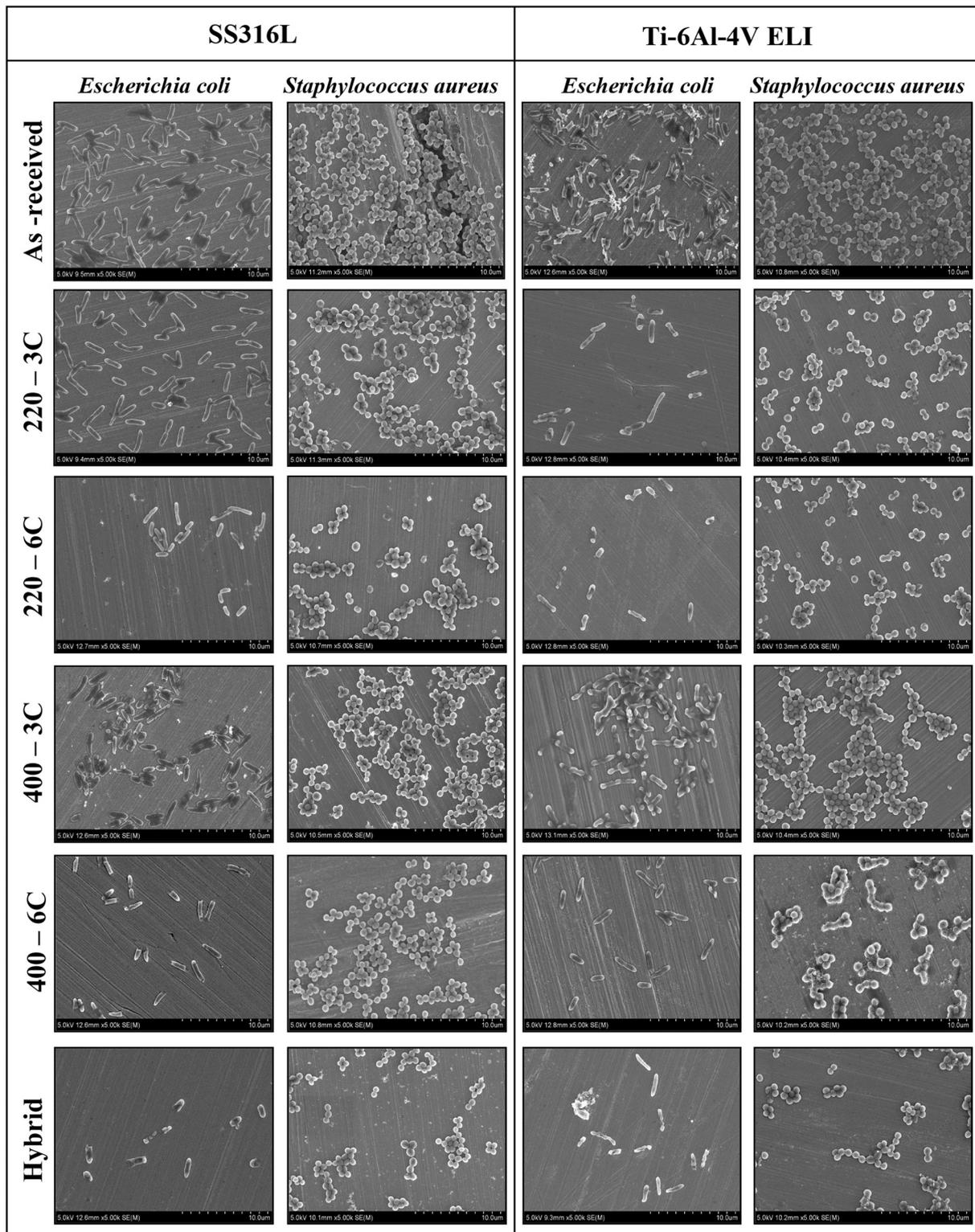
Fig. 14. SEM images of bacterial adhesion on samples.

surfaces are unexplored and is needed in the future study.

4. Conclusions

Unidirectional abrasive flow finishing is one step process in which complex internal and external shapes including freeform surfaces can be finished to nano level roughness with controlled topography without damaging to the dimensional accuracy. In this process viscoelastic

polymer based abrasive media is used to finish the surfaces, it is a mixture of polymer, plasticizer, and abrasive particles. In this paper, an attempt has been made to demonstrate the possibility to finish the biomaterials to the nano level using the developed process which may reduce the bacterial adhesion to the implant surface. Following conclusions are drawn from the present study:

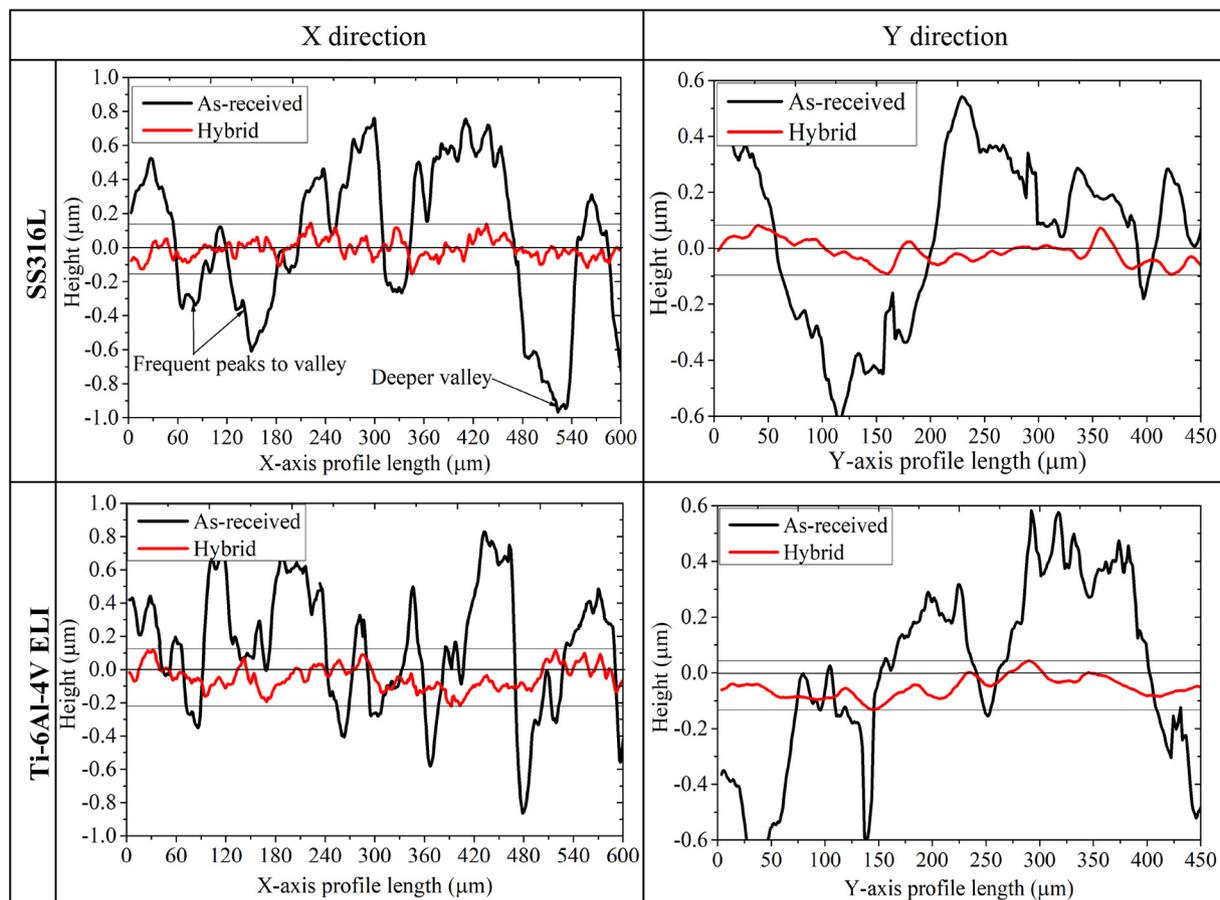• The average surface roughness (R_a) of the SS316L as-received

Fig. 15. Comparison of 2D roughness profile.

sample is 463 nm ± 20 nm. After finishing with abrasive media of 220 mesh size at 3 cycles, it is reduced to 163 nm ± 15 nm and another 3 cycles, again it reduces to 113 nm ± 12 nm. Similar trend is observed for all the samples finished with different parameters.

- Change in surface roughness of the SS316L and Ti-6Al-4 V ELI is observed as the number of finishing cycles increases. Minimum roughness 68 nm and 73 nm for SS316L and Ti-6Al-4 V ELI are achieved on the surfaces finished with hybrid parameters.
- Bearing area curve shows as the finishing progress, the density of the peaks and valleys reduces. Contact angle measurement showed that finishing process increases the contact angle from 88.5° ± 3.6° to 102° in case of SS316L and for Ti-6Al-4 V ELI contact angle increased from 83° ± 6° to 96° ± 4°.
- Bacterial adhesion study shows that the bacteria adhesion reduces with reduced surface roughness and also found that fewer bacteria adherence on the finished surfaces.
- Morphological features of the surfaces are also an important parameter to be considered while quantifying the bacteria adhesion because colonies of bacteria are found more in the grooves and crevices present over the surfaces.

The approach presented in this work shows the ability of the process in tailoring the surface roughness and surface topography of the surface. Although the bacterial adhesion is reduced on the finished surfaces compared to the as-received surface, further tuning of the process parameters is needed.

Conflict of Interest

The authors have no conflicts of interest to declare.

Acknowledgment

References

[1] M.J. Lysaght, J.A. O'Loughlin, Demographic scope and economic magnitude of contemporary organ replacement therapies, ASAIO J. 46 (2000) 515–521, https://doi.org/10.1097/00002480-200009000-00001.

[2] M. Ribeiro, F.J. Monteiro, M.P. Ferraz, Infection of orthopedic implants with emphasis on bacterial adhesion process and techniques used in studying bacterial-material interactions, Biomatter 2 (2012) 176–194, https://doi.org/10.4161/biom.22905.

[3] M. Navarro, A. Michiardi, O. Castano, J. Planell, Biomaterials in orthopaedics, J. R. Soc. Interface 5 (2008) 1137–1158, https://doi.org/10.1098/rsif.2008.0151.

[4] D. Choudhury, M. Vrbka, A. Bin Mamat, I. Stavness, C.K. Roy, R. Mootanah, I. Krupka, The impact of surface and geometry on coefficient of friction of artificial hip joints, J. Mech. Behav. Biomed. Mater. 72 (2017) 192–199, https://doi.org/10.1016/j.jmbbm.2017.05.011.

[5] T.F. Moriarty, R. Kuehl, T. Coenye, W.-J. Metsemakers, M. Morgenstern, E.M. Schwarz, M. Riool, S.A.J. Zaat, N. Khana, S.L. Kates, R.G. Richards, Orthopaedic device-related infection: current and future interventions for improved prevention and treatment, EFORT Open Rev. 1 (2016) 89–99, https://doi.org/10.1302/2058-5241.1.000037.

[6] C.R. Arciola, D. Campoccia, G.D. Ehrlich, L. Montanaro, Biofilm-based implant infections in orthopaedics, Adv. Exp. Med. Biol. 830 (2015) 29–46, https://doi.org/10.1007/978-3-319-11038-7.

[7] H. Koseki, A. Yonekura, T. Shida, I. Yoda, H. Horiuchi, Y. Morinaga, K. Yanagihara, H. Sakoda, M. Osaki, M. Tomita, Early staphylococcal biofilm formation on solid orthopaedic implant materials: in vitro study, PLoS One 9 (2014) e107588, , https://doi.org/10.1371/journal.pone.0107588.

[8] C.W. Chan, L. Carson, G.C. Smith, A. Morelli, S. Lee, Enhancing the antibacterial performance of orthopaedic implant materials by fibre laser surface engineering, Appl. Surf. Sci. 404 (2017) 67–81, https://doi.org/10.1016/j.apsusc.2017.01.233.

[9] M. Hocevar, M. Jenko, M. Godec, D. Drobne, An overview of the influence of

stainless-steel surface properties on bacterial adhesion, Mater. Tehnol. 48 (2014) 609–617 (doi:669.14.018.8:620.179.11).

[10] Y.H. An, R.J. Friedman, Handbook of Bacterial Adhesion, Humana Press, New Jersey, 2000, https://doi.org/10.1385/1592592244.

[11] S.C. Cox, P. Jamshidi, N.M. Eisenstein, M.A. Webber, H. Burton, R.J.A. Moakes, O. Addison, M. Attallah, D.E.T. Shepherd, L.M. Grover, Surface finish has a critical influence on biofilm formation and mammalian cell attachment to additively manufactured prosthetics, ACS Biomater. Sci. Eng. 3 (2017) 1616–1626, https://doi.org/10.1021/acsbiomaterials.7b00336.

[12] F. Song, H. Koo, D. Ren, Effects of material properties on bacterial adhesion and biofilm formation, J. Dent. Res. 94 (2015) 1027–1034, https://doi.org/10.1177/0022034515587690.

[13] K. Bohinc, G. Dražić, A. Abram, M. Jevšnik, B. Jeršek, D. Nipič, M. Kurinčič, P. Raspor, Metal surface characteristics dictate bacterial adhesion capacity, Int. J. Adhes. Adhes. 68 (2016) 39–46, https://doi.org/10.1016/j.ijadhadh.2016.01.008.

[14] A. Turger, J. Köhler, B. Denkena, T.A. Correa, C. Becher, C. Hurschler, Manufacturing conditioned roughness and wear of biomedical oxide ceramics for all-ceramic knee implants, Biomed. Eng. Online 12 (2013) 84, https://doi.org/10.1186/1475-925X-12-84.

[15] C.W. Kang, F.Z. Fang, State of the art of bioimplants manufacturing: part I, Adv. Manuf. 6 (2018) 20–40, https://doi.org/10.1007/s40436-017-0207-4.

[16] S.S. Kumar, S.H. Somashekhar, Finishing of Multiple Components and Surface Characterization, vol. 5, (2017), pp. 1–8.

[17] J. Kenda, J. Duhovnik, J. Tavcar, J. Kopac, Abrasive flow machining applied to plastic gear matrix polishing, Int. J. Adv. Manuf. Technol. 71 (2014) 141–151, https://doi.org/10.1007/s00170-013-5461-4.

[18] A.M. Sidpara, V.K. Jain, Nanofinishing of freeform surfaces of prosthetic knee joint implant, Proc. Inst. Mech. Eng. Part B J. Eng. Manuf. 226 (2012) 1833–1846, https://doi.org/10.1177/0954405412460452.

[19] T.S. Kavithaa, N. Balashanmugam, Nanometric surface finishing of typical industrial components by abrasive flow finishing, Int. J. Adv. Manuf. Technol. 85 (2016) 2189–2196, https://doi.org/10.1007/s00170-016-8486-7.

[20] V.K. Jain, S.G. Adsul, Experimental investigations into abrasive flow machining (AFM), Int. J. Mach. Tools Manuf. 40 (2000) 1003–1021, https://doi.org/10.1016/S0890-6955(99)00114-5.

[21] S.S. Kumar, S.H. Somashekhar, Effect of surface roughness and surface topography on wettability of machined biomaterials using flexible viscoelastic polymer abrasive media, Surf. Topogr. 7 (2019) 015004, , https://doi.org/10.1088/2051-672X/aaf6f6.

[22] ASTM F138-13a, Standard Specification for Wrought 18Chromium-14Nickel-2.5Molybdenum Stainless Steel Bar and Wire for Surgical Implants (UNS S31673), ASTM International, West Conshohocken, PA, 2013.

[23] ASTM F136-13, Standard Specification for Wrought Titanium-6Aluminum-4Vanadium ELI (Extra Low Interstitial) Alloy for Surgical Implant Applications (UNS R56401), ASTM International, West Conshohocken, PA, 2013.

[24] B. Bhushan, Introduction to Tribology, Wiley, New York, 2013.

[25] M. Kanthababu, M.S. Shunmugam, M. Singaperumal, Identification of significant parameters and appropriate levels in honing of cylinder liners, Int. J. Mach. Mach. Mater. 5 (2009) 80–96, https://doi.org/10.1504/IJMMM.2009.023114.

[26] R. Laheurte, P. Darnis, N. Darbois, O. Cahuc, J. Neauport, Subsurface damage distribution characterization of ground surfaces using Abbott–Firestone curves, Opt. Express 20 (2012) 13551–13559, https://doi.org/10.1364/OE.20.013551.

[27] J. Loberg, I. Mattisson, S. Hansson, E. Ahlberg, Characterisation of titanium dental implants I: critical assessment of surface roughness parameters, Open Biomater. J. 2 (2010) 18–35, https://doi.org/10.2174/1876502501002010018.

[28] K.J. Stout, Development of Methods for the Characterisation of Roughness in Three Dimensions, Penton Press and Contributors London, 2004.

[29] M. Quirynen, C.M.L. Bollen, The influence of surface roughness and surface-free energy on supra- and subgingival plaque formation in man, J. Clin. Periodontol. 22 (2005) 1–14, https://doi.org/10.1111/j.1600-051X.1995.tb01765.x.

[30] T. Wassmann, S. Kreis, M. Behr, R. Buergers, The influence of surface texture and wettability on initial bacterial adhesion on titanium and zirconium oxide dental implants, Int. J. Implant Dent. 3 (2017) 32, , https://doi.org/10.1186/s40729-017-0093-3.

[31] C.M.L. Bollenl, P. Lambrechts, M. Quirynen, Comparison of surface roughness of oral hard materials to the threshold surface roughness for bacterial plaque retention: a review of the literature, Dent. Mater. 13 (1997) 258–269, https://doi.org/10.1016/S0109-5641(97)80038-3.

[32] L.B. Hauslich, M.N. Sela, D. Steinberg, G. Rosen, D. Kohavi, The adhesion of oral bacteria to modified titanium surfaces : role of plasma proteins and electrostatic forces, Clin. Oral Implants Res. 24 (2013) 49–56, https://doi.org/10.1111/j.1600-0501.2011.02364.x.

[33] I. Yoda, H. Koseki, M. Tomita, T. Shida, H. Horiuchi, H. Sakoda, M. Osaki, Effect of surface roughness of biomaterials on Staphylococcus epidermidis adhesion, BMC Microbiol. 14 (2014) 234, , https://doi.org/10.1186/s12866-014-0234-2.

[34] M. Katsikogianni, Y. Missirlis, Concise review of mechanisms of bacterial adhesion to biomaterials and of techniques used in estimating bacteria-material interactions, Eur. Cells Mater. 8 (2004) 37–57, https://doi.org/10.22203/eCM.v008a05.

[35] K.J. Edwards, A.D. Rutenberg, Microbial response to surface microtopography: the role of metabolism in localized mineral dissolution, Chem. Geol. 180 (2001) 19–32, https://doi.org/10.1016/S0009-2541(01)00303-5.

[36] M. Lorenzetti, I. Dogša, T. Stošicki, D. Stopar, M. Kalin, S. Kobe, S. Novak, The influence of surface modification on bacterial adhesion to titanium-based substrates, ACS Appl. Mater. Interfaces 7 (2015) 1644–1651, https://doi.org/10.1021/am507148n.

[37] M.E. Barbour, D.J. O'Sullivan, H.F. Jenkinson, D.C. Jagger, The effects of polishing methods on surface morphology, roughness and bacterial colonisation of titanium abutments, J. Mater. Sci. Mater. Med. 18 (2007) 1439–1447, https://doi.org/10.1007/s10856-007-0141-2.

[38] C.J. Mortimer, L. Burke, C.J. Wright, Microbial interactions with nanostructures and their importance for the development of electrospun nanofibrous materials used in regenerative medicine and filtration, J. Microb. Biochem. Technol. 8 (2016) 195–201, https://doi.org/10.4172/1948-5948.1000285.